Indian Journal of Engineering & Materials Sciences
Vol. 30, August 2023, pp. 614-621
DOI: 10.56042/ijems.v30i4.2520

Design and Analysis of 2D Photonic Biosensor with ML for Respiratory Virus Detection

Vishalatchi S[a], Kalpana Murugan[a*], Nagaraj R[b] & Gayathri H N[c]
[a]Department of Electronics and Communication Engineering, Kalasalingam Academy of Research and Education, Srivilliputhur 626 126, India
[b]Mohan Babu University, Tirupati 517 102, India
[c]Department of Chemistry, The Oxford College of Engineering, Bengaluru 560 068, India

Received: 09 June 2023; Accepted: 05 August 2023

In this study, we have designed and integrated a novel photonic biosensor with a Machine Learning approach for the detection of five common respiratory viruses. The biosensor has been developed using a two-dimensional hexagonal photonic crystal defect structure, which has been designed through the use of Finite Difference Time Domain (FDTD) and Plane Wave Expansion (PWE) techniques to monitor wavelength shifts during virus detection. The analytes have been efficiently captured within the sensor's pores to optimize performance. The uniqueness of our sensor has been demonstrated through enhanced sensitivity (584nm/RIU) and a remarkable quality factor (9734). We have employed the naïve Bayes classifier Machine Learning algorithm to achieve accurate virus detection, leveraging parameters that have been extracted from the sensor design. Our integrated sensor and classifier have provided robust classification of virus types, outperforming existing methods, and yielding highly accurate results. Furthermore, to enhance user accessibility, we have developed a graphical user interface for intuitive result interpretation.

Keywords: Naïve Bayes, Sensor, Virus, 2D PhC, Hexagonal ring resonator, Sensitivity, Quality factor, Respiratory virus

1 Introduction

Viruses have long been acknowledged as perilous parasitic entities with the capacity to infect living organisms, giving rise to a broad spectrum of diseases. These infectious agents, characterized by their minuscule size and uncomplicated composition, have exclusively targeted living cells[1]. Within the host organism, viruses have thrived, replicated, and at times, rendered traditional antibiotic treatments ineffective. The primary objective of this study has been to introduce a highly sensitive sensor device capable of exceptionally accurate detection of the presence of viruses in blood samples[2]. Specifically, our focus has encompassed five viruses that frequently afflict the respiratory system: Influenza[3], Corona[4], Adeno[5], HBoV (Human Boca virus)[6], and Tuberculosis[7]. The consequences of respiratory infections[8] have been severe, potentially leading to fatal outcomes if not promptly detected and treated.

In recent years, the world has borne witness to the emergence of new and more menacing viruses, resulting in global pandemics. As Selma Souf has noted, viruses pose the most dangerous threats to human life[9], leading to grave health concerns. Innovative technologies, such as the Europium Nanoparticle-based Immune Assay (ENIA), have been developed for detecting Influenza A and B viruses in blood samples. Similar approaches have been employed to identify respiratory viruses, including swine-origin influenza A/H1N1 and SARS coronavirus. These endeavors underscore the paramount importance of early virus detection, which has been achieved through the utilization of a Photonic crystal environment.

A Photonic Biosensor is an established analytical device designed to detect analytes by amalgamating a reactive element with a physical and chemical indicator. The term "biosensors" was first introduced by Clark and Lyons in the 1960s. These sensors can be categorized as tissue-based, enzyme-based, or magneto/piezo-electric based sensors. Within these sensors, biological analytes have been recognized for their ability to modify the properties of light particles, encompassing the light source, waveguide medium, and photodetector[10]. Recently, ring resonators have gained prominence due to their diminutive size and prompt responsiveness. Two-dimensional photonic

*Corresponding author (E-mail:drmkalpanaece@gmail.com)

crystal defect engineering[11] has played a pivotal role in achieving optimal sensor performance.

Two configurations of 2D photonic crystals, involving rods in an air format and holes in a slab format as defined in Fig. 1, have been meticulously studied to ascertain band gap values and key parameters, such as sensitivity, transmission spectrum, and quality factor, through the introduction of defects[12]. These defects have enabled the formation of resonators and waveguide structures, which, in this study, have assumed the form of two unique designs. These structures have been realized using waveguides and multiple ring resonators, potentially integrating into future circuit systems[13]. They have facilitated repetitive analysis of biological samples on a single chip. Photonic technology, with its advantages in light transmission and Terahertz range data transmission, has played a pivotal role in enhancing sensor performance. Silicon, a reliable light medium, has been harnessed to capture photon energy, often combined with Sio2 pores to achieve precise wavelength accommodation.

Machine learning[14] has played a pivotal role in improving system accuracy and surmounting the limitations associated with less sensitive and less accurate devices[15]. In data analysis, classification has been a fundamental task, entailing the assignment of data instances to predefined classes based on attribute sets. Supervised classification has entailed constructing classifiers using labeled data sets, where each data point has been accurately assigned to a specific class. This has culminated in the creation of a model for class distribution. Our approach has harnessed the naive Bayes classifier, consistently demonstrating high accuracy and precision scores.

In contemporary times, the most significant causes of deadly diseases have been attributed to the introduction of viruses into the environment, posing serious threats to human health. According to the World Health Organization (WHO), most deaths have resulted from respiratory viruses present in society, with the most common culprits being Corona, Influenza, Tuberculosis, Adeno, and HBoV. Statistical reports have emphasized the paramount role of early virus detection[16] in preventing fatalities. The primary objectives of this paper have been to address these challenges by achieving high sensitivity and accuracy.

2 Materials and Methods

In this section, two dimensional photonic crystal biosensor mechanism has been modelled using Maxwell's equation and the Machine learning part has been done by naïve Bayes classifier technique which are clearly explained further.

2.1 2D Photonic Biosensor

The transmission spectrum of light in a photonic crystal, Plane-wave expansion and Finite Difference Time Domain method are the major categories involved in the primary analysis. The superposition of a set of plane waves, Propagation modes and bandgap attain an accurate solution by having the PWE method. The FDTD method can be utilized by Maxwell's equation to achieve the field distribution, power transmission and transmission spectra. In the photonic crystal, these Maxwell's equations play a role in the analysis of electromagnetic wave propagation. It can be normally expressed as

$$\frac{\partial H}{\partial t} = \frac{1}{\mu}\nabla \times E \qquad ...(1)$$

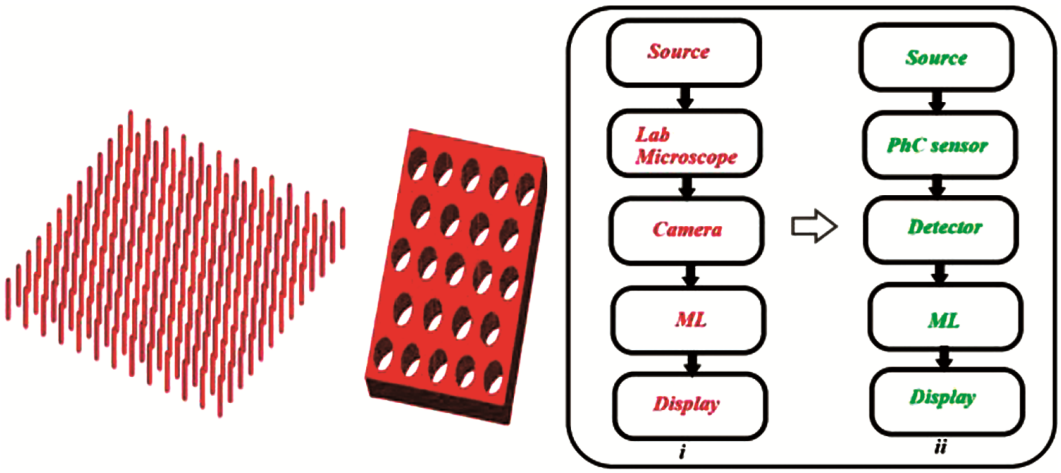

Fig. 1 — The basic 2D photonic crystal structure for rods and holes and (i) Schematic diagram of existing work, & (ii) schematic diagram of proposed work.

$$\frac{\partial E}{\partial t} = \frac{1}{\varepsilon}\nabla \times H \quad ...(2)$$

Maxwell's equation can be solved with the help of bandgap diagrams in an electric field which is noted by,

$$\nabla \times \left(\frac{1}{\varepsilon(r)}\nabla \times E(r)\right) = \frac{\omega^2}{c^2}E(r) \quad ...(3)$$

ω is the angular frequency, ε(r) is relative permittivity, E(r) is the electric field of the periodic function and c is the speed of light. The propagation of light can be implied by using the overhead equation. The Bloch theorem describes that electromagnetic wave propagation can be deprived of scattering in periodic media. The dielectric constant can be modified due to the use of periodic 2D photonic crystal and the ε can be rewritten as,

$$\nabla \times \left(\frac{1}{\varepsilon(r)}\nabla \times E(r+R)\right) = \frac{\omega^2}{c^2}E(r+R) \quad ...(4)$$

R represents the 2D lattice vector. The solutions to the periodic Eigen value problem can be done by the Bloch theorem which can be stated as,

$$H_k(r) = e^{ikr}u_k(r) \quad ...(5)$$

$$(ik+\nabla) \times \frac{1}{\varepsilon(r)}(ik+\nabla) \times u_k(r) = \frac{\omega(k)^2}{c^2}u_k(r) \quad ...(6)$$

$u_k(r)$ is a lattice periodic function. The band diagram might be generated by skimming the Bloch vector, k over the Brillouin zone.

The Finite Difference Time Domain method can be utilized for the analysis of the transmission spectrum and can be transferred below,

$$E_x\Big|_{i,j}^{n+1} = E_x\Big|_{i,j}^{n} + \frac{c\Delta t}{\varepsilon_0}\left[\frac{H_z\Big|_{i,j+1/2}^{n+1/2} - H_z\Big|_{i,j+1/2}^{n+1/2}}{\Delta_y}\right] \quad ...(7)$$

$$E_y\Big|_{i,j}^{n+1} = E_y\Big|_{i,j}^{n} - \frac{c\Delta t}{\varepsilon_0}\left[\frac{H_z\Big|_{i+1/2,j}^{n+1/2} - H_z\Big|_{i-1/2,j}^{n+1/2}}{\Delta_y}\right] \quad ...(8)$$

$$H_z\Big|_{i,j}^{n+1/2} = E_z\Big|_{i,j}^{n-1/2} + \frac{c\Delta t}{\mu_0}\left[\frac{E_x\Big|_{i,j+1/2}^{n} - E_x\Big|_{i,j-1/2}^{n}}{\Delta_y}\right] - \left[\frac{E_y\Big|_{i+1/2,j}^{n} - E_y\Big|_{i+1/2,j}^{n}}{\Delta_x}\right] \quad ...(9)$$

Where n indicates a discrete-time step, i and j can be noted as discrete grid points in the X and Y plane. The following condition intimates the relation between temporal and spatial step size to attain a stable simulation.

$$\Delta t \leq \frac{1}{c\sqrt{\frac{1}{\Delta x^2}+\frac{1}{\Delta y^2}}} \quad ...(10)$$

where c denotes the light speed. It is mainly based on the Fourier transform.

2.2 Performance Metrics

Q factor and sensitivity are the deciding functions to identify the better performance of the sensor. The quality factor is defined as the ratio of Δλo (resonant wavelength) concerning λ_{FWHM} (Full Width Half Maximum).

$$Quality\ Factor = \frac{\Delta\lambda_\circ}{\lambda_{FWHM}} \quad ...(11)$$

The Sensitivity is defined as the change in maximum resonant wavelength shift to the change in refractive index as

$$S = \frac{\Delta\lambda}{\nabla n} \quad ...(12)$$

Where Δλ, the change is in resonant wavelength shift and is a change in refractive index.

2.3 ML with Photonics

The data collected from the photonic sensor device are trained and tested by using ML technique known as naïve Bayes classifier and it classifies the given data according to the trained and tested one.

The naive Bayes classifier is an addendum with probability models with selection criteria[17]. Among the many common rules, one rule that stands out is to pick the most probable hypothesis; this is known as the MAP (maximum a posterior) decision rule[18]. The corresponding classifier, a Bayes classifier, is the function that assigns a class label ŷ = Ck for some k as follows:

$$\hat{y} = \underset{k\epsilon\{1,\ldots m\}}{argmax}\, p(C_k)\prod_{i=1}^{n} p(a_i|C_k) \quad ...(13)$$

3 Results and Discussion

Here, the Photonic sensor has been designed with suited specification and chosen parameters are eligible to provide mode polarization and Photonic Band Gap. The Bio sensing mechanism of PhC are further discussed in detailed manner

3.1 Design specification

The generated 2D crystal sensors are based on a hexagonal ring resonator structure with a linear line defect in it. It is formed by having circular holes or

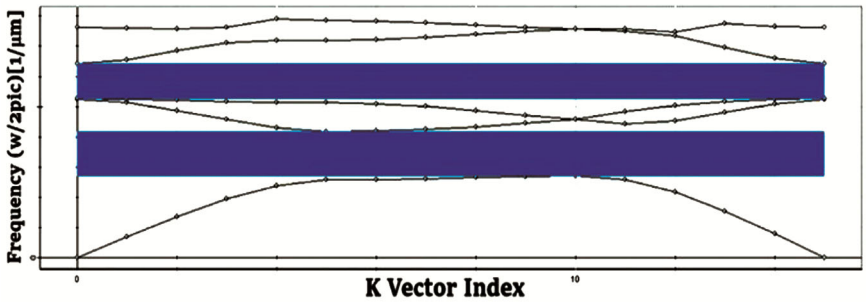

Fig. 2-The photonic bandgap for TE mode structure.

pits in the wafer module. The radius of the holes is classified into two categories that provide holes at the corners are having a smaller radius of r=0.09 µm and the remaining radius of holes as r=0.13 µm. The analyte can be placed at the linear position of the sensor resonator. These holes are aligned in a periodic hexagonal array. These alignments can be done by achieving meritorious control TE and TM propagation mode and reduction of dispersion take place with a higher bandgap. The hexagonal ring resonator structures are composed of 29 holes in the x-direction and 31 holes in the Z direction. The distance between the holes is 0.45µm.

3.2 PBG calculation

In the 2D crystal, when the light starts its confinement within the crystal, a difficulty arises for the entire propagation. These struggles can be overcome by making defects in the structured crystal. The periodical structure is broken for the easy propagation of EM (Electro-Magnetic) waves throughout the PBG zone. It is very needful for the intact transfer of the signal after the defect insertion through a reformed crystal structure.

The PBG (Photonic Band Gap) calculation is carried out using the PWE method for distinct transverse polarizations in Electric and Magnetic as TE (Transmission Electric and TM (Transmission Magnetic) modes.

In the TE mode of polarization, two higher band gaps are obtained. The initial PBG lies between 0.54397 and 0.83439, which relates to the next PBG as 1.05512 and 1.27999 1/λ shown in Fig. 2 are known as optical transmission windows for the performance of the sensor. The three-dimensional electric field distribution can play a major role in the formation of the bandgap structure shown in Fig .3

3.3 Biosensing mechanism

The mechanism explains the performance of following two sensors

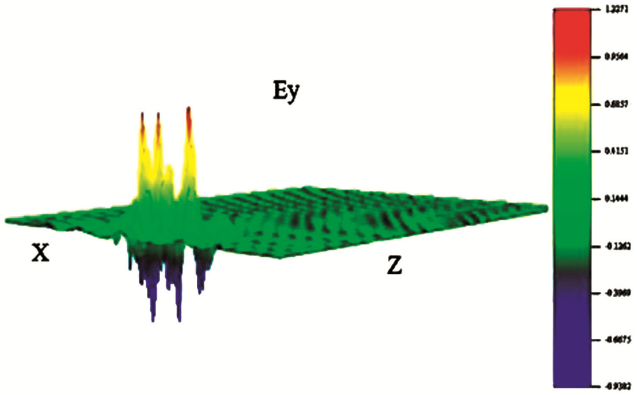

Fig. 3 — The 3D Electric field distribution of 2DPCHRR.

Figure 4 explain the structure of the double horizontal ring resonator which has unique properties and characteristics in terms of the result obtained. It has its comparison among themselves in the form of quality factor, sensitivity and amplitude of transmission spectrum. Here the mechanism has been known for selecting four holes in the waveguide and reducing the radius in the corner of the designed one.

Figure 5 depits the double vertical hexagonal ring resonator structures which are designed to attain the comparison among the older ones and worked to attain maximum quality factor, sensitivity and amplitude shown.

3.4 Bio sensing outcome

Transmission spectra of 2D Photonic Crystal Hexagonal Double Horizontal Ring Resonator Sensor (2DPCHDHRR) and 2D Photonic Crystal Hexagonal Double Vertical Ring Resonator Sensor (2DPCHDHRR) are discussed here,

The graph in Fig. 6 explains the wavelength shift of the double horizontal hexagonal ring resonator sensor. The double horizontal hexagonal ring resonator sensor has sensitivity values of 516nm, 429nm, 582nm, 415nm, and 564nm for Influenza, Corona, TB, Adenovirus and HBoV respectively and the

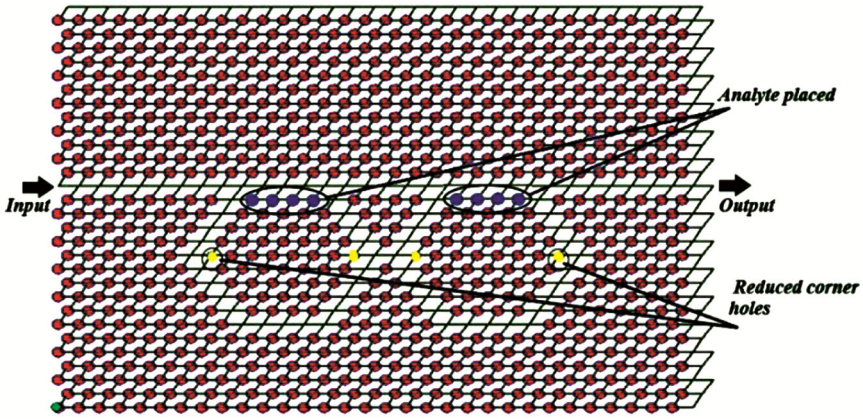

Fig. 4 — Structure of 2D Photonic Crystal HexagonalDouble Horizontal Ring Resonator Sensor(2DPCHDHRR).

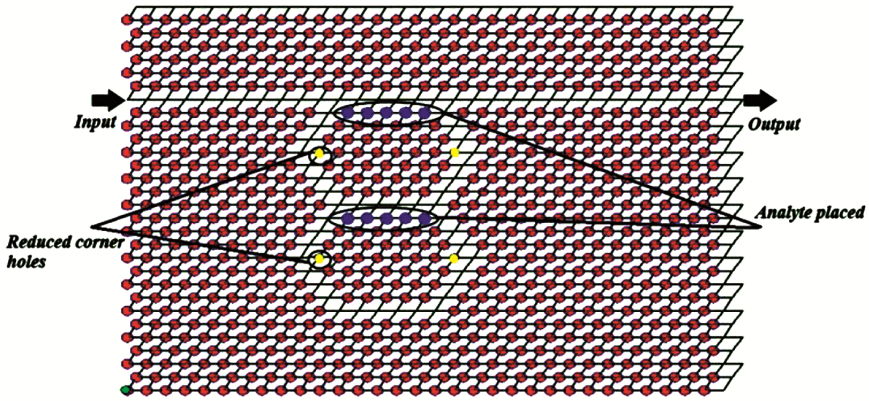

Fig. 5 — Structure of 2D Photonic Crystal Hexagonal Double Vertical Ring Resonator Sensor(2DPCHDVRR).

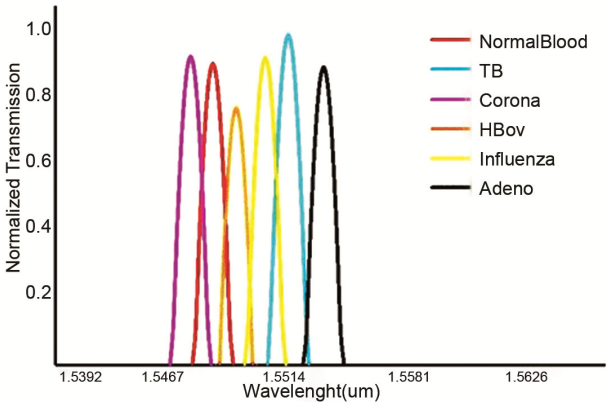

Fig. 6 — Transmission spectra of 2D Photonic Crystal Hexagonal Double Horizontal Ring Resonator Sensor (2DPCHDHRR).

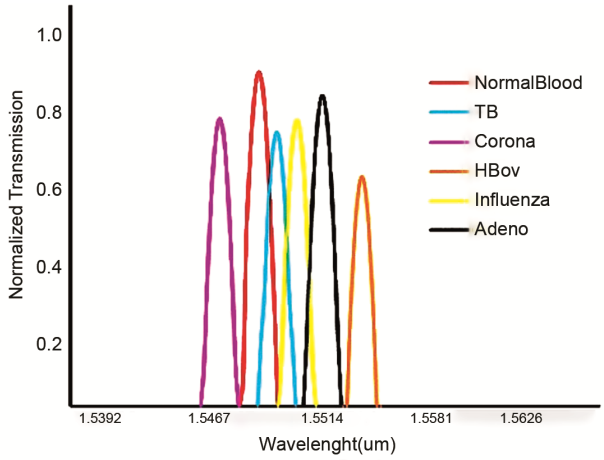

Fig. 7 — Transmission spectra of 2D Photonic Crystal Hexagonal Double Vertical Ring Resonator Sensor (2DPCHDHRR).

quality factor for Normal cell, Influenza, Corona, TB, Adenovirus and HBoV as 8673, 8964, 9348, 9734, 8549 and 7971 respectively.

The graph in Fig. 7 explains the wavelength shift of the double vertical hexagonal ring resonator sensor. The double vertical hexagonal ring resonator sensor has sensitivity values of 289nm, 208nm, 333nm, 295nm and 221 nm for Influenza, Corona, TB, Adenovirus and HBoV respectively and the quality factor for Normal cell, Influenza, Corona, TB, Adenovirus and HBoV as 8532, 7934, 7795, 7459,8358 and 7204 respectively.

Table 1 is considered the refractive index dataset used for the detection process. Table 2 shows the amplitude, quality factor and sensitivity of the infected cells compared with the normal cells for the

double horizontal hexagonal ring resonator sensor. In this sensor design, the higher-level sensitivity obtained for the double horizontal hexagonal ring resonator sensor is 582nm and the quality factor is 9734.

Table 3 shows the amplitude, quality factor and sensitivity of the infected cells compared with the normal cells for the double vertical hexagonal ring resonator sensor. In this sensor design, the higher level sensitivity obtained for the double vertical hexagonal ring resonator sensor is 333nm and the quality factor is 8532.

Table 4 explains the reported values of the present work in the form of sensitivity and quality factors by comparing it with the existing work of the same and proved that our proposed work attained higher values.

Table 1 — Refractive index values of the virus

Name of the cell	Refractive Index
Normal	1.3459
Influenza	1.48
Corona	1.06
Adeno	1.376
TB	1.352
HBoV	1.364

Table 2 — The functional parameters of the 2d phc hexagonal double horizontal ring resonator sensor

Name of the cell	Amplitude	Quality Factor	Sensitivity (nm)
Normal	0.896	8673	***
Influenza	0.914	8964	516
Corona	0.925	9348	429
TB	0.997	9734	582
Adeno	0.869	8549	415
HBoV	0.732	7971	564

Table 3 — The functional parameters of the 2d phc hexagonal double vertical ring resonator sensor

Name of the cell	Amplitude	Quality Factor	Sensitivity (nm)
Normal	0.912	8532	***
Influenza	0.779	7934	289
Corona	0.794	7795	208
TB	0.741	7459	333
Adeno	0.836	8358	295
HBoV	0.618	7204	221

Table 4 — The reported higher quality factor and sensitivity value compared with existing work

References	Year	Sensitivity (nm)	Quality factor
20	2015	***	3700
13	2020	210	6776
22	2020	550	***
21	2021	143	248
Present work	2023	582	9734

Figures 8 and 9 talk about the average variation that takes place between yearly progress for sensitivity and quality factors.

3.5 Classification results

Here, Machine learning technique known as naïve Bayes classification yields the classified results that has sensor inputs and classified outputs that are discussed further in sub sections

The sensor produces the outcome of different signatures in terms of wave length[23] and transmission spectrum which have few changes by using the various refractive index. The attributes are extracted from the OptiFDTD tool and the classifier is used for data classification.

Technically, we have extracted the above observations in the .csv format and have used the python pre-defined libraries for Machine Learning to classify the data using Naïve Bayes classifier at the back end and a responsive Html page onthe front end has been designed to display the results based on the training and testing data input provided as shown in Fig. 10 and Fig. 11. From the above classification process, we have obtained an accuracy of 95.7 %.

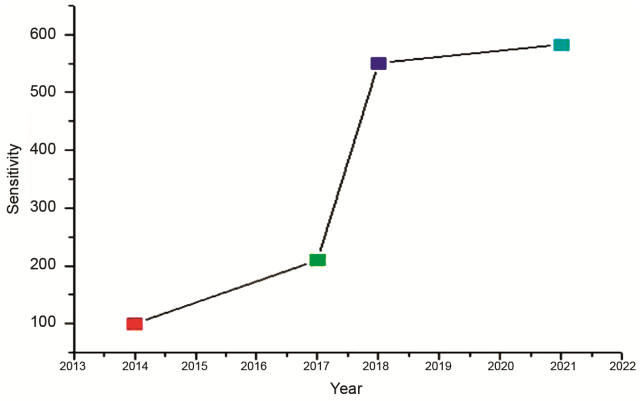

Fig. 8 — Sensitivity graph concerning the year.

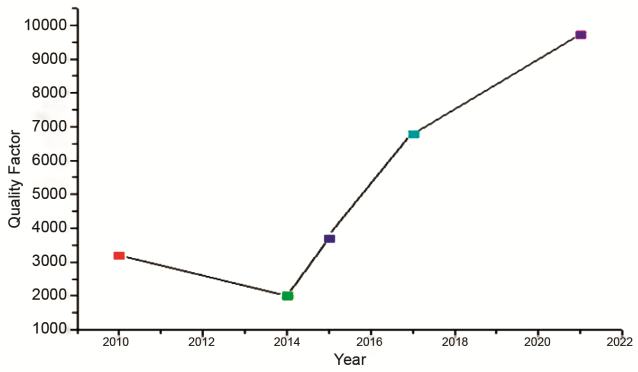

Fig. 9 — Quality factor graph concerning the year.

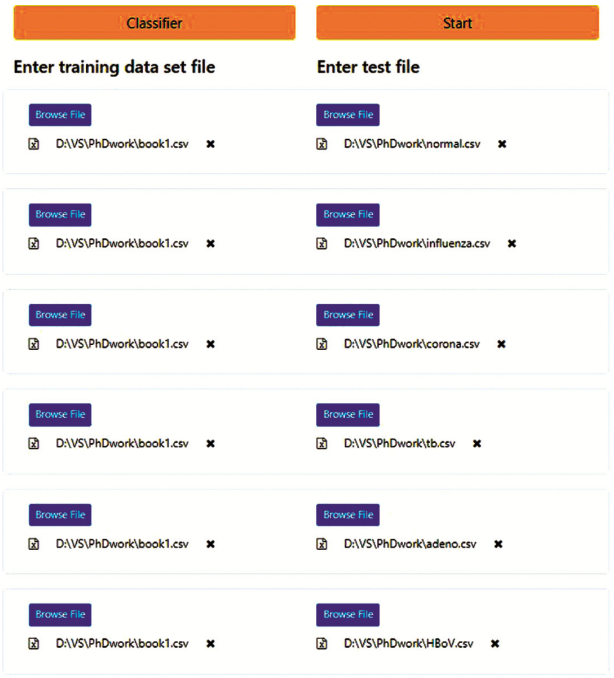

Fig. 10 — Allow training and test data upload for data classification.

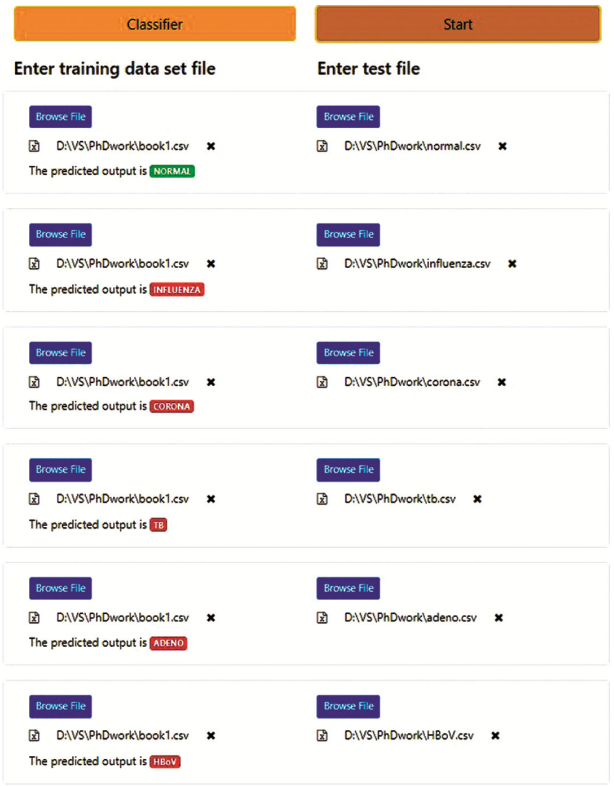

Fig. 11 — Response after analyzing the input data.

4 Conclusion

In this work, two categories of 2D photonic hexagonal ring resonator sensors and their comportment have been premeditated. Among the comparison of two sensors, the best one has been found and it is 2D PhC Hexagonal Double Horizontal Ring Resonator Sensor the sensor design has high sensitivity and quality factors can be further used for fabrication process in future. The effective refractive index change of the sensing hole plays a major role in the bio-sensing mechanism. The bounded molecules of analytes in the sensing hole produce effective resonant wavelength shift which is mainly based on higher dependence on the sensing hole position and undeviating link with change in refractive index. The quality factor reaches the value of about 9734 and the sensitivity keeps a high value of about 582nm. Table 2 is the assurance that a comparative study of our work leads to good sensitivity and quality factors. The whole architecture indicates an efficient way of exposing high sensitivity and quality factors by analyzing various virus analytes in two forms of similar classifications of sensor design. By regulating the defects in the crystal and reducing the corner radius placed, the following advantages can be obtained including small scale in sensor array and recognizing numerous bio sensing mechanisms without any crosstalk

The proposed sensor design structures with unique specifications are further utilized for photonic integrated circuits. The fabrication of the selected design can be imposed for the process in real-time applications for the detection of virus analytes present in the human blood. The miniature nature of the device and low cost makes the sensor more reliable and efficient. It involves less amount of testing samples for the detection process and also the response will be very fast. The designs are modified for improving the sensing performance and hence used for the micro and macro level fabrication. The photonics market is estimated to embellish over the forecast period.

Acknowledgement

We would like to say thanks to one and all helped to complete this paper by giving proper guidance. Also we wish to thank all the staff of the research and development center, for sharing resources and suggested ideas with immense knowledge for accomplishing the research work by providing essential tools.

References

1 Yolles M, Frieden R,*Systems,*10(3) (2022) 70.
2 Sharma T, Vasisht P, Vashishath M,*Int j inf tecnol,* 13 (2021) 983.

3 Vemula S V, Zhao J, Liu J, Wang X, Biswas S, Hewlett I, *Viruses*,8(4) (2016) 96.
4 Fahim M, Ghonim HAES, Roshdy W H, et al, *JMIR Public Health Surveill*, 7(4) (2021) 27433.
5 Lynch JP 3rd, Kajon A E, *Semin Respir Crit Care Med*, 37(4) (2016) 586.
6 Wang X, Stelzer-Braid S, Scotch M, Rawlinson W D, *Reviews in Medical Virology*, 32(5) (2022) 2375.
7 Utomo B, Chan C K, Mertaniasih N M, Soedarsono S, *Tropical Medicine and Infectious Disease*, 7(6) (2022) 83.
8 Yamin, M, *Int j inf Tecnol*, 10 (2018)503.
9 Selma Souf, *The International Journal of Student Research*, 9 (2016) 32.
10 Altug H, Oh S H, Maier S A, *Nat Nanotechnol*, 17 (2022)5.
11 Kumar H, Nikhil BK & Sreerangaraju MN, *Int j tecnol*, 13, (2021) 613.
12 Sundaresan V S, Ramrao N, *2021 8th Int Conf on Computing for Sustainable Global Development (INDIACom)*, 2021 720.
13 Ajey S S, Bhanumathi, H R, Srikanth, P C , *Int j inf tecnol*, 12 (2020) 1393.
14 Shaikh A, Sharan P, Srikanth P C, *Int j inf tecnol*, 13 (2021) 785.
15 Chakraborty S, Jana GC, Kumari D, *Int j inf tecnol,* 12 (2020) 473.
16 Khanday A M U D, Rabani S T, Khan Q R, *Int j inf tecnol,* 12 (2020) 731.
17 Sundaresan V S, Ramrao N, Sharan P, & Murugan K, *IJEMS*, 28 (2021) 209.
18 Nehal SA, Roy D, Devi M, *Int j inf tecnol,* 12 (2020) 495.
19 Sharma, A, Mishra PK, *Int j inf tecnol*, 14 (2022) 1949.
20 Harhouz A, Hocini A, *J Electromagnet Waves Appl,* 29(5) (2015) 659.
21 Kumar BMH, Srikanth PC & Vaibhav AM, *Int j inf tecnol*, 13 (2021) 2053.
22 Kumar B M, Vaibav A M, SrikanthP C, *CONCEECT,* 2020.
23 Petrov, Dmitry, *J of Quantitative Spectroscopy and Radiative Transfer*, 248 (2020)107005.